Bioactive Materials 40 (2024) 334–344

Contents lists available at ScienceDirect

Bioactive Materials

journal homepage: www.keaipublishing.com/en/journals/bioactive-materials

Wet tissue adhesive polymeric powder hydrogels for skeletal muscle regeneration

Mingyu Lee [a,1], Daun Seo [a,1], Junggeon Park [a], Sun Hong Lee [b], Jin Jeon [b], Woochan Kim [c,d,e], Jangho Kim [c,d,e], Hee Seok Yang [b], Jae Young Lee [a,*]

[a] School of Materials Science and Engineering, Gwangju Institute of Science and Technology, Gwangju, 61005, Republic of Korea
[b] Department of Nanobiomedical Science & BK21 FOUR NBM Global Research Center for Regenerative Medicine, Dankook University, Cheonan, 31116, Republic of Korea
[c] Department of Convergence Biosystems Engineering, Chonnam National University, Gwangju, 61186, Republic of Korea
[d] Department of Rural and Biosystems Engineering, Chonnam National University, Gwangju, Republic of Korea
[e] Interdisciplinary Program in IT-Bio Convergence System, Chonnam National University, Gwangju, 61186, Republic of Korea

ARTICLE INFO

Keywords:
Powder
Hydrogel
Wet-adhesive
Skeletal muscle regeneration

ABSTRACT

Volumetric muscle loss (VML) frequently results from traumatic incidents and can lead to severe functional disabilities. Hydrogels have been widely employed for VML tissue regeneration, which are unfortunately ineffective because of the lack of intimate contact with injured tissue for structural and mechanical support. Adhesive hydrogels allow for strong tissue connections for wound closure. Nevertheless, conventional adhesive hydrogels exhibit poor tissue adhesion in moist, bleeding wounds due to the hydration layer at the tissue–hydrogel interfaces, resulting in insufficient performance. In this study, we developed a novel, biocompatible, wet tissue adhesive powder hydrogel consisting of dextran-aldehyde (dex-ald) and gelatin for the regeneration of VML. This powder absorbs the interfacial tissue fluid and buffer solution on the tissue, spontaneously forms a hydrogel, and strongly adheres to the tissue via various molecular interactions, including the Schiff base reaction. In particular, the powder composition with a 1:4 ratio of dex-ald to gelatin exhibited optimal characteristics with an appropriate gelation time (258 s), strong tissue adhesion (14.5 kPa), and stability. Dex-ald/gelatin powder hydrogels presented strong adhesion to various organs and excellent hemostasis compared to other wet hydrogels and fibrin glue. A mouse VML injury model revealed that the dex-ald/gelatin powder hydrogel significantly improved muscle regeneration, reduced fibrosis, enhanced vascularization, and decreased inflammation. Consequently, our wet-adhesive powder hydrogel can serve as an effective platform for repairing various tissues, including the heart, muscle, and nerve tissues.

1. Introduction

Skeletal muscle constitutes approximately 30–40 % of body weight and is primarily responsible for body movement and force generation. Skeletal muscle is frequently damaged to diverse degrees by trauma [1,2]. Traumatic incidents often result in volumetric muscle loss (VML), with a loss of >20 % of the total skeletal muscle mass, which leads to irreversible muscle loss, impaired functionality, and long-term disability [3]. The current clinical standard for VML treatment is autologous muscle flap transplantation; however, it has several critical drawbacks, including complicated surgical procedures, limited donor site availability, and incomplete functional restoration [4,5]. Hence, a simple and effective therapeutic approach to promote skeletal muscle regeneration in VML is urgently required.

Biomaterial-based treatments have emerged for effective skeletal muscle repair [6], as these materials can provide a structural and mechanical environment for VML regeneration. Biomaterials can transduce force in injured muscles, reduce fibrosis, and induce muscle regeneration [5,7,8]. In particular, materials with good biocompatibility, biodegradability, and tissue-like mechanical properties are favored for

Peer review under responsibility of KeAi Communications Co., Ltd.
* Corresponding author.
E-mail address: jaeyounglee@gist.ac.kr (J.Y. Lee).
[1] These authors contributed equally.

https://doi.org/10.1016/j.bioactmat.2024.06.017
Received 23 December 2023; Received in revised form 24 May 2024; Accepted 10 June 2024

facilitating regeneration of injured muscles. Hydrogels have been widely studied as biomimetic materials for tissue engineering because of their beneficial characteristics such as high hydration, softness, and interconnecting porosity. Hydrogels can be tailored further with specific functionalities, such as biodegradability and adhesiveness, for specific tissue regeneration [9–12]. Tissue-adhesive hydrogels, in particular, enable stable and strong contact with target tissues, which are especially beneficial for applications involving tissues in dynamic movements (e.g., skeletal muscle) and wound closure [13–15]. For muscle regeneration, adhesive hydrogels can offer stable muscle connections between muscle fibers, which enable proper force transduction and regeneration. However, conventional adhesive hydrogels frequently lose their adhesiveness in wet environments (hemorrhage and biological fluid) because the hydration layer at the tissue–hydrogel interface impedes firm tissue adhesion.

Recently, powder hydrogels that eliminate the hydration layer at tissue interfaces by absorbing interfacial water have been developed to achieve wet-tissue adhesion [16–18]. The resultant hydrogels could strongly adhere to the tissues and provide stable and intimate support for tissue regeneration. Powder hydrogels offer several benefits for tissue regeneration, including fast and large-volume removal of a hydration layer on the tissue and adaptability to irregularly shaped wound sites with conformal contact. Several studies have demonstrated the utility of powder hydrogels for the regeneration of various tissues. Peng et al. synthesized polyethyleneimine/polyacrylic acid (PEI/PAA) powder for the in situ formation of physical hydrogels on wet tissue and demonstrated excellent wet-tissue adhesiveness and regeneration of gastrointestinal perforations [18]. However, these synthetic polymers (PEI and PAA) are non-biodegradable and do not form strong covalent bonds with tissues, raising concerns regarding their potential toxicity and instability. In addition, its stability and performance in dynamic environments, including skeletal muscles, remain unexplored. Consequently, the development of powder hydrogels with good biocompatibility, biodegradability, and reliable and strong adhesion to dynamic wet tissues is highly desired.

Several studies demonstrated the effectiveness of wet-adhesive hemostatic powders for treating non-compressible and bleeding wounds using diverse materials, such as carboxymethyl chitosan/aldehyde-modified hyaluronic acid grafted with catechol groups, oxidized dextran/methacrylate gelatin, and benzeneboronic acid-modified sodium alginate/catechol-modified quaternized chitosan [19–21]. These powders showed excellent shape adaptability and hemostatic efficacy. However, most studies have focused solely on the hemostatic performance for bleeding wounds and have not explored their applicability for tissue regeneration. Importantly, powders consisting of highly-modified polymers may raise serious concerns regarding toxicity, side reactions, and difficulties in synthesis and purification affecting reproducibility. To address these issues, our study developed a wet-tissue adhesive polymeric powder hydrogel by combining biocompatible natural polymers, specifically dextran-aldehyde (dex-ald) and gelatin, aimed at skeletal muscle regeneration after VML. Dex-ald was synthesized through a simple modification process and formulated with gelatin to finally produce dex-ald/gelatin powder. The dex-ald/gelatin powder absorbs interfacial tissue fluid and spontaneously forms an in situ hydrogel via the Schiff base reaction between dex-ald and gelatin on a tissue. Furthermore, this powder hydrogel can strongly adhere to tissues primarily via covalent Schiff base formation between the hydrogels and tissues. We systematically investigated the influence of powder composition and treatment procedures on material properties such as mechanical, rheological, and adhesion. Furthermore, the in vivo performance of the powder hydrogel was assessed using various organs, specifically examining the adhesion strength and hemostatic ability, which were compared with those of other wet hydrogels and fibrin glue. Finally, the feasibility of the powder hydrogel for skeletal muscle regeneration was demonstrated using an animal VML model.

2. Materials and methods

2.1. Materials

Gelatin from porcine skin (gel strength ~300 g bloom, type A), dextran from *Leuconostoc* spp. (average molecular weight 450,000–650,000 Da), sodium periodate ($NaIO_4$), ethylene glycol, hydroxylamine hydrochloride ($NH_2OH{\cdot}HCl$), sodium bicarbonate ($NaHCO_3$), sodium dodecyl sulfate (SDS), glycine, and anti-von Willebrand factor (vWF) rabbit polyclonal antibody (AB7356) were purchased from Sigma-Aldrich (St. Louis, MO, USA). Dulbecco's Modified Eagle Medium (DMEM), fetal bovine serum (FBS), and Dulbecco's Phosphate-Buffered Saline (DPBS) were purchased from HyClone (Logan, UT, USA). Antibiotic-antimycotic (100 × ; penicillin 10,000 units/mL, streptomycin 10,000 μg/mL, amphotericin 25 μg/mL), trypsin/EDTA (0.05 %), Live/Dead viability/cytotoxicity kit for mammalian cells, 2,4,6-trinitrobenzene sulfonic acid (TNBSA) 5 % w/v solution, Pacific Hemostasis® Thromboplastin-DS solution (FSD100354), and Pacific Hemostasis® APTT-XL solution (FSD100403) were purchased from Thermo Fisher Scientific (Waltham, MA, USA). Ez-Cytox Wst-1 (4-[3-(4-iodophenyl)-2-(4-nitro-phenyl)-2H-5-tetrazolio]-1,3-benzene sulfonate) assay kit was purchased from DoGenBio (Seoul, Republic of Korea). Masson's trichrome staining kit was purchased from BBC Biochemical (Mount Vernon, WA, USA). Alexa fluor 488 (goat anti-rat) IgG (H + L) and Alexa fluor 555 (goat anti-rabbit) IgG (H + L) were purchased from Molecular Probes (Eugene, OR, USA). *Anti*-F4/80 rat monoclonal antibody (ab6640), anti-mannose (CD206) rabbit polyclonal antibody (ab64693) and Picro-sirius red stain kit (ab150681) were purchased from Abcam (Cambridge, UK). *Anti*-α-smooth muscle actin (α-SMA) was purchased from Cell Signaling Technology Inc. (Danvers, MA, USA).

2.2. Preparation of polymeric powder hydrogel

2.2.1. Synthesis and characterization of dex-ald

Dex-ald was synthesized by oxidizing dextran according to a previously literature [22]. In brief, 5 g of dextran was completely dissolved in 500 mL of deionized (DI) water at 25 °C. $NaIO_4$ (2.673 g) was dissolved in 20 mL DI water. The $NaIO_4$ solution was added dropwise to the dextran solution with vigorous stirring. This mixture was further incubated in the dark with stirring at 25 °C for 2 h. Ethylene glycol (0.695 mL) was added to the mixture solution for 1 h to stop the reaction. The solution was dialyzed using a 3500 Da membrane (Spectrum Laboratories Inc., TX, USA) in DI water for 3 days. After dialysis, the solution was filtered through a 0.2-μm filter and lyophilized. Chemical modification of dextran to dex-ald was examined by H^1-NMR spectroscopy (Fig. S1). The aldehyde groups in the synthesized dex-ald were determined using a hydroxylamine hydrochloride titration assay [22]. Briefly, 0.1 g of dex-ald was dissolved in 10 mL of 0.025 M $NH_2OH{\cdot}HCl$ solution and stirred for 1 h. The solution was titrated using 0.1 M NaOH. Then, the aldehyde group content in dex-ald was determined to be 3.48 mmol/g according to the following equation, which corresponded to a degree of substitution of 58.5 %.

$$\text{Aldehyde group content (mmol / g)} = \frac{mmol\ of\ aldehyde\ group}{gram\ of\ dex-ald}$$

2.2.2. Molecular weight measurement

The weight average molecular weights (Mw) and polydispersity (PDI) of dextran, dex-ald, and gelatin were determined using gel permeation chromatography equipped with a multi-angle light-scattering detector (miniDAWN TREOS, Wyatt Technology Co., CA, USA) and a refractive index detector (RI2012A, Schambeck SFD, Germany) (Table S1). The Mws of dextran, dex-ald, and gelatin were 3.69 ± 0.03 × 10^5, 4.65 ± 0.26 × 10^4, and 3.69 ± 0.05 × 10^5 g/mol, respectively. The PDIs (Mw/Mn) of dextran, dex-ald, and gelatin were 1.02 ± 0.01,

1.07 ± 0.08, and 1.57 ± 0.08, respectively.

2.2.3. Quantification of amine group in gelatin

The amine content in gelatin was quantified using a TNBSA solution following the manufacturer's instructions. Briefly, gelatin was dissolved in 0.1 M sodium bicarbonate (pH 8.5) at a concentration of 20 μg/mL. Standard solutions were prepared using glycine at concentrations ranging from 20 to 0.625 μg/mL. TNBSA was diluted to 0.01 % using sodium bicarbonate solution and mixed with 0.5 mL of the sample or standard solution. After incubation at 37 °C in a shaking incubator for 2 h, 0.25 mL of 10 % SDS and 0.125 mL of 1 N HCl were added to each mixture. The absorbance of each solution was measured at 335 nm using a UV–vis spectrometer (Touch Duo, Biodrop, Cambridge, UK).

2.2.4. Preparation of dex-ald/gelatin powder

Lyophilized dex-ald (0.2 g) and gelatin (0.8 g) were mixed together in a 50 mL conical tube and ground using a homogenizer (IKA T10 basic, IKA Works Inc., Staufen, Germany) at 25 °C for 10 min. The particulate dex-ald/gelatin powders were refined using a sieve (50 mesh, Chunggye Sieve Co., Ltd., Seoul, Republic of Korea) to remove particles >300 μm in size. The prepared powders were transferred to petri dishes and exposed to ultraviolet light for 4 h for sterilization. For powder hydrogel formation, dex-ald/gelatin powders were placed at the site of interest, then 1x PBS (at 37 °C) was added and incubated for 5 min to allow gelation.

2.3. Characterization of polymeric powder hydrogels

2.3.1. Mechanical properties

The mechanical properties of the hydrogels were analyzed using an oscillatory rheometer (Kinexus; Malvern Instruments, Worcestershire, UK). For the time-sweep test, shear moduli of individual samples were measured at a frequency of 1 Hz with a strain of 0.5 % at 37 °C for 30 min. The gelation time of the dex-ald/gelatin powder hydrogel was determined as the time when the decreasing shear modulus (G′) began to increase after PBS addition to the powder. In the frequency-sweep test, shear moduli of samples were measured in a frequency range of 0.1–10 Hz with 0.5 % strain at 37 °C. Young's modulus was calculated using the shear storage modulus obtained at a frequency of 1 Hz [23].

2.3.2. Adhesion properties

The adhesion strength of the powder hydrogels was evaluated by measuring the lap shear stress using a universal testing machine (TO-100-IC; Testone, Gyeonggi, Republic of Korea). For adhesion tests, porcine skin was cut into 0.2-cm-thick rectangular pieces (4.0 cm × 1.5 cm). Dex-ald/gelatin powder was placed on the skin tissue, hydrated by addition of PBS (3 mL PBS at 37 °C per g powder) onto the powder, immediately covered with another skin tissue, and incubated at 37 °C for 30 min. Note that the gel/tissue contact area was set to approximately 1.5 cm × 1.0 cm. For the tensile tests, both ends of the powder hydrogel-loaded tissue samples were fixed to individual clamps and stretched at a rate of 2 mm/min using a 10 kN load cell. To examine hydrogel-tissue adhesion under dynamic conditions, the powder hydrogel was formed on porcine skin tissue by PBS treatment (3 mL PBS per g powder) to the powder and incubation at 37 °C for 5 min as described earlier. The adhesion and stability of the hydrogel-loaded tissues were examined under various deformations such as twisting, bending, and exposure to water flushing.

2.4. In-vitro cell studies

2.4.1. C2C12 cell culture

Mouse C2C12 myoblasts were cultured in tissue culture plates (TCPs) in a growth medium (high glucose DMEM supplemented with 10 % FBS and 1 % antibiotic-antimycotic solution [100 X]) at 37 °C with 5 % CO_2. When the myoblasts reached 70–80 % confluence on TCPs, the cells were detached using a 0.05 % (w/v) trypsin/EDTA solution. Myoblasts were then seeded in 24-well plates at a density of 2×10^4 cells/cm^2 and incubated in growth medium for an additional 24 h before culture with the hydrogels. The medium was changed every day.

2.4.2. Cytocompatibility test

The cytocompatibility of the powder hydrogels was examined by in vitro C2C12 cell culture in both direct and indirect contact modes. First, a disc-shaped powder hydrogel was prepared by hydrating 30 mg of sterile dex-ald/gelatin powder in 24 well plates with sterile PBS (3 mL PBS per g powder) and incubated at 37 °C for 3 h. For a direct contact culture, the hydrogel disc was carefully placed on the cells growing on TCP. For indirect hydrogel culture, the hydrogel was placed on the upper part of a transwell insert, while cells were cultured on the bottom part.

The cytocompatibility of a sample was assessed by live/dead cell staining and metabolic activity assays following the manufacturers' instructions. For live/dead cell staining, an assay solution was prepared by adding 2 μL of 2 mM EthD-1 and 0.5 μL of 5 mM calcein AM to 1 mL DPBS. The cell culture medium and hydrogel were removed, and the assay solution was added to each culture plate. After incubation for 10 min, the cells were washed twice with sterile DPBS for 5 min each. Fluorescence images were acquired using a fluorescence microscope (Leica DMI 3000 B). The numbers of live (green) and dead (red) cells were counted from random fluorescence images using ImageJ software (NIH, Bethesda, MD, USA). Cell viability was reported as the percentage of live cells among the total (live and dead) cells, according to the following equation:

$$\textit{Cell viability}\ (\%) = \frac{\textit{The nunmer of live cells}}{\textit{The number of total cells}} \times 100(\%)$$

The metabolic activity of the cells was measured using the WST-1 assay. Briefly, the culture medium in each well was replaced with fresh medium during cell culture, and WST solution was added to the medium at a 10:1 ratio (culture medium: WST solution). After a 1.5 h incubation at 37 °C, 100 μL of the culture medium was transferred to a 96-well plate. The absorbance was measured at 450 nm using a microplate reader (Varioskan LUX, Thermo Fisher Scientific, Waltham, MA, USA). The WST-1 assay was performed daily for 3 days.

2.5. In vivo studies

2.5.1. Animal care and experimentation

All animal studies were reviewed and approved by the Animal Care and Use Committees (ACUC) of the Gwangju Institute of Science and Technology, Republic of Korea (approval number: GIST-2023-041), and all experiments were performed after approval by the local ethics committee at Gwangju Institute of Science and Technology. Six-week-old male BALB/c mice (weight 20–23 g) and 8-week-old male Sprague–Dawley rats (weight 200–230 g) were purchased from Orient Bio Inc. (Seoul, Republic of Korea). Mice and rats were anesthetized with 2 % and 3 % isoflurane (Ankuk Inc., Republic of Korea), respectively, for the following in vivo experiments.

2.5.2. In vivo adhesion and hemostatic test

The adhesion to various organs and hemostatic ability of the hydrogels were tested using various experimental hydrogel groups, including 'fibrin glue', 'pre-formed hydrogel', 'in situ-formed hydrogel', and 'dex-ald/gelatin powder hydrogel groups. For the pre-formed hydrogel group, 1-mm thick rectangular hydrogels were prepared by incubating 2.5 wt% dex-ald and 10 wt% gelatin in PBS for 24 h at 37 °C using a PDMS mold and then applied to each organ. For the in situ hydrogel group, 5 wt% dex-ald and 20 wt% gelatin solutions (in PBS) were mixed in a 1:1 vol ratio using a static mixing needle (Nordson EFD, OH, USA) and a dual syringe, and applied to each organ. For the fibrin glue group, the fibrin glue (Greenplast, Greencross Corporation, Seoul, Republic of Korea) was applied directly to each organ. For the dex-ald/

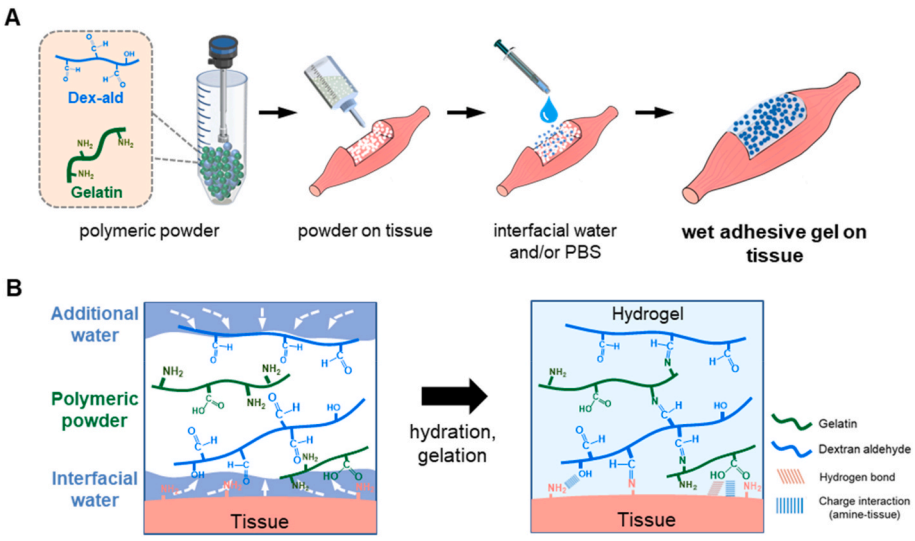

Fig. 1. Schematic representation of a wet adhesive dex-ald/gelatin powder hydrogel. (A) Hydration and gelation processes of the dex-ald/gelatin powder hydrogel. (B) Crosslinking and tissue adhesion of the dex-ald/gelatin powder hydrogel during and after hydration.

gelatin powder hydrogel group, the dex-ald/gelatin powder was directly applied to each organ. For the adhesion test, PBS (3 mL PBS per g powder) was added to the powder on an organ.

The following five organs were used for the in vivo adhesion tests: three non-bleeding organs (liver, stomach, and intestine) in rats, the hemorrhagic heart in rats, and the hemorrhagic tibialis anterior (TA) muscle with VML injury in mice. The liver, stomach, intestine, and heart of rats were exposed via an abdominal incision. Hemorrhagic rat hearts were induced by a 3-mm incision in the epicardium of the left ventricle with a surgical blade. The hemorrhagic mouse TA muscle with VML injury was prepared by removing a 3-mm thick piece (5 mm × 3 mm) from the TA muscle using sterile forceps and surgical scissors. In each organ, 100 mg of hydrogel was applied and incubated for 5 min. For the powder hydrogel group, 25 mg of dex-ald/gelatin powder was applied to each organ and hydrated with PBS (3 mL PBS per g powder). For tissue adhesion stability tests, the hydrogels on tissues were splashed with 1 × saline for 10 s in a squeeze bottle. A mouse hemorrhagic liver model was established to study the hemostatic ability of individual samples. The mouse liver was exposed through an abdominal incision, and a filter paper was placed under the liver with a plastic bag on the back of the filter paper to prevent the absorption of other fluids. A piece of liver (5 mm × 5 mm) was cut and removed to allow bleeding, and 12.5 mg of dex-ald/gelatin powder or 100 mg of the other hydrogels (fibrin glue, preformed-hydrogel, and in situ hydrogel) was immediately applied to the bleeding site to examine hemostasis. The untreated group was used as a control. Blood loss was calculated by measuring the weight of the filter paper before and after blood adsorption (3 min) in each group.

2.5.3. Establishment of VML injury and treatment with the dex-ald/gelatin powder hydrogel

VML injury was established by removing the TA muscle from the mice. A 1-cm-long incision was carefully made on the lateral aspect of the lower leg. The skin was gently separated from the fascia by blunt dissection. A piece of the TA muscle (1 mm in thickness and 5 mm × 2 mm in size) was carefully excised using sterile forceps and surgical scissors. The cavity was then filled with each sample. The experimental groups comprised untreated (PBS), fibrin glue, and a dex-ald/gelatin powder hydrogel. For the untreated group, 20 μL of PBS was added into the injury and incubated for 5 min. For the fibrin glue group, 20 μL of fibrin glue was loaded onto the wound and allowed to gel for 5 min. For the dex-ald/gelatin hydrogel group, 5 mg of sterile powder was placed onto the wound, followed by addition of 15 μL of sterile PBS on the powder and 5 min incubation. Skin was then sutured for closure in each group. Five animals were used for each experiment.

2.5.4. Histological analysis

One and three weeks after VML injury and sample treatment, the TA muscle was removed, fixed using formalin, and embedded in paraffin blocks. Hematoxylin and eosin (H&E) staining was performed according to a previously reported protocol [24]. Masson's trichrome (MT) staining and Picro-sirius red staning were performed according to the manufacturer's instructions. Optical microscopy images of the stained tissue sections were acquired using a VS200 Research Slide Scanner (OLYMPUS, Tokyo, Japan). For the H&E-stained images, the area of the centronucleated muscle fibers was measured using the ImageJ software. Fibrotic areas were measured from the blue-stained fibrosis deposits in the MT-stained images using the ImageJ software. The percentage of fibrotic area was calculated as the fibrotic area divided by the injured area. For immunohistochemical analysis, tissue slides were treated with 10 mM citrate buffer (pH 6.0) and incubated at 98 °C for 15 min for antigen retrieval. The samples were incubated in blocking solution (3 % normal goat serum in DPBS) at 25 °C for 1 h and incubated in primary antibody solution (F4/80 and CD206 or vWF or α-SMA, respectively; 1:100 dilution in blocking solution) at 4 °C overnight. The section samples were washed three times with PBS and incubated in secondary antibody solution (Alexa fluor® 488 and Alexa fluor 555 or Alexa fluor® 555, respectively; 1:200 dilution in the blocking solution) at 25 °C for 1 h. Fluorescence images were acquired using a fluorescence microscope (Leica DMI 3000 B).

2.6. Statistical analysis

All experiments were conducted in triplicates unless otherwise specified. Statistical significance was determined using one-way analysis of variance (ANOVA) with Tukey's post-hoc comparison of mean values. Statistical analyses were performed using Origin Pro 2021 (9.8) software (OriginLab Corp., OH, USA), with a significance level of 0.05.

3. Results and discussion

3.1. Preparation of dex-ald/gelatin powder hydrogel

Dex-ald/gelatin powder was prepared by mixing and homogenizing lyophilized dex-ald and gelatin (Fig. 2A). After homogenization, the powder was sieved using a 300-μm sieve. Dex-ald powder had a short, fragmented fiber shape, and gelatin powder exhibited a spherical

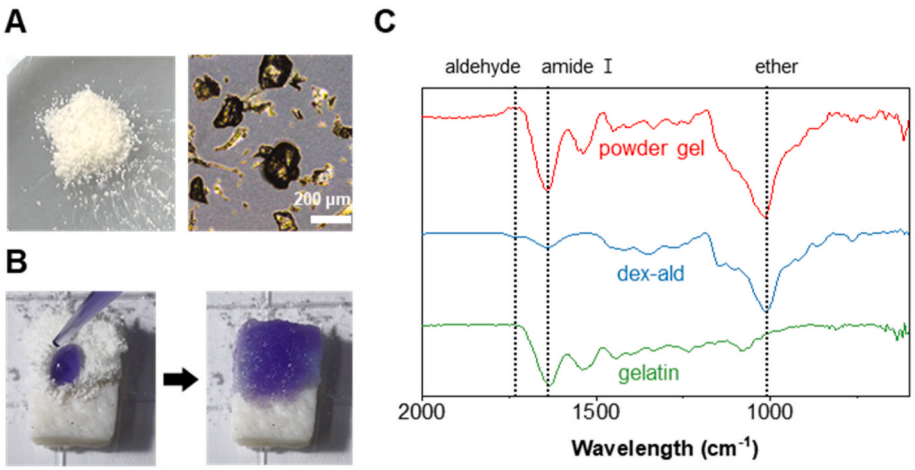

Fig. 2. Composition and characteristics of dex-ald/gelatin powder. (A) Photograph and optical micrograph of the powder. (B) Powder hydrogel formed on porcine skin tissue by PBS addition (supplemented with blue dye for visualization). (C) Fourier-transform infrared (FTIR) spectra of gelatin, dex-ald, and powder (dex-ald/gelatin) hydrogel. Dex-ald/gelatin powder prepared at a weight ratio of 1:4 (dex-ald:gelatin) was used.

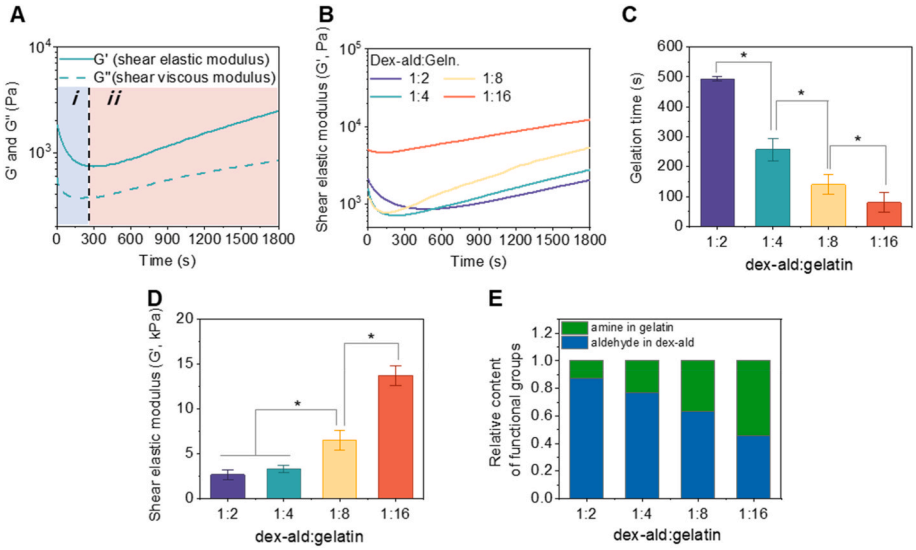

Fig. 3. Mechanical characterization of dex-ald/gelatin powder hydrogels with different ratios (1:2, 1:4, 1:8, and 1:16) of dex-ald and gelatin. Each powder was hydrated by the addition of 3 mL PBS per g powder. (A) Time-dependent shear elastic and viscous moduli of the power hydrogel prepared with dex-ald and gelatin at a 1:4 wt ratio - *i*) hydration phase after PBS treatment and *ii*) gelation phase. G′ and G″ indicate an elastic component and a viscous component of the shear modulus, respectively. (B) Time-dependent shear elastic moduli (G′) of the power hydrogels after PBS treatment. (C) Gelation times of the hydrogels. (D) Shear elastic moduli (G′) of the hydrogels 30 min after incubation in PBS. (E) Relative amine and aldehyde contents of powders. Statistical significance was analyzed by one-way ANOVA followed by a Tukey analysis. $*p < 0.05$.

morphology (Fig. S2). The small particle size of the powder was expected to have a large surface area for rapid fluid adsorption, leading to fast hydration and gelation (Fig. 2B). The hydrated powder forms a hydrogel by spontaneous Schiff base formation between gelatin and dex-ald and strongly binds to tissues via non-covalent interactions (e.g., hydrogen bonding and electrostatic interactions) and covalent Schiff base reactions between dex-ald and proteins in the tissue (Fig. 1B). Because the interfacial water is mostly removed by the powder, no hydration layer remains at the tissue/hydrogel interface, which enables the adhesive functional groups of the powder (e.g., aldehyde, carboxyl, amine, and hydroxyl groups) to effectively react and bind to the tissue. Owing to these characteristics, the dex-ald/gelatin powder hydrogel can strongly adhere to wet tissues. The powder hydrogel formed by treatment with PBS was examined by FT-IR spectroscopy (Fig. 2C). Dex-ald and gelatin exhibited characteristic aldehyde peak at 1735 cm^{-1} and amide bond peak at 1633 cm^{-1} [25,26]. (Fig. 2C). In the dex-ald/gelatin hydrogel spectrum, a new peak corresponding to Schiff base appeared at 1056 cm^{-1}, and the aldehyde peak at 1735 cm^{-1} diminished [27], implying successful Schiff base formation in the hydrogel. In addition, scanning electron micrographs of the powder hydrogels showed the porous structures of typical hydrogels (Fig. S3). After further incubation, the hydrogel presented relatively uniform pores, implying an eventual crosslinking reaction and a uniform internal structure.

3.2. Mechanical characterization of dex-ald/gelatin powder hydrogel

Various dex-ald/gelatin powders were formulated by varying the ratio of dex-ald to gelatin (1:2, 1:4, 1:8, and 1:16), which were termed as powder (1:2), powder (1:4), powder (1:8), and powder (1:16), respectively, and their rheological properties were characterized (Fig. 3). First, the rheological behavior of the powder hydrogels was monitored after PBS treatment in time-sweep mode (Fig. 3A and B). Interestingly, two

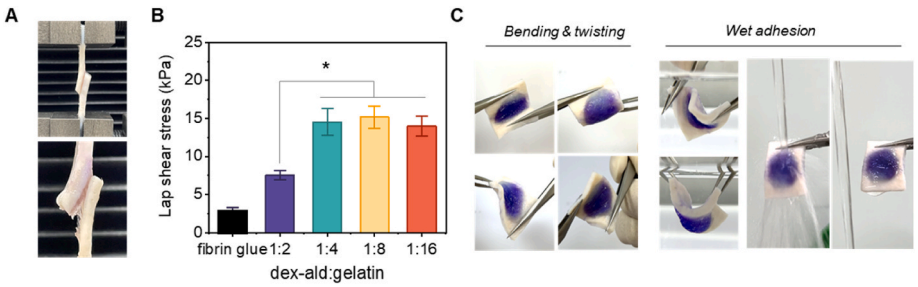

Fig. 4. Adhesion properties of the dex-ald/gelatin powder hydrogels with different ratios (1:2, 1:4, 1:8, and 1:16) of dex-ald/gelatin. (A) Photographs of the lap-shear test of the powder (1:4) hydrogels using porcine skin tissues. (B) Adhesive strengths of the powder hydrogels. The fibrin glue group was tested as a control group. (C) Photographs of the powder (1:4) hydrogel on porcine skin under dynamic deformation conductions (bending and twisting) and wet environment (twisting in water and water flushing). Statistical significance was analyzed by one-way ANOVA followed by Tukey analysis * $p < 0.05$.

different modulus trends were observed after PBS addition – (*i*) an initial modulus decrease and (*ii*) a gradual modulus increase. For this observation, we speculated two events that the powder might undergo: (*i*) initial powder hydration with decreasing modulus and (*ii*) eventual crosslinking (gelation) with increasing modulus. The elastic modulus (G') remained higher than viscous modulus (G″) throughout both hydration and gelation periods, indicating the powder hydrogel dominantly exhibits gel-like behaviors. Since the powers quickly absorb solution, the swollen powders may exhibit gel-like mechanical behaviors even at an early hydration stage. Granular hydrogels (composed of hydrated microgels) typically show higher G' than G'' even without strong interparticle interactions [28,29]. In our powder hydrogel system, an addition of a small amount of solution leads to fast swelling of individual powers. These swollen hydrogels undergo internal crosslinking within the individual particles and eventually interparticle crosslinking during the gelation phase, forming a monolithic hydrogel (Fig. S4). The gelation time of the powder hydrogel was determined as the time at which the modulus began to increase. Rapid hydration and gelation of a powder are important in in-vivo applications. When gelation occurs too slowly in a wound, the powder may leak from the wound with body fluids before appropriate gelation. In our study, the powders containing a higher ratio of gelatin exhibited faster hydration and shorter gelation times (Fig. 3C). The powder (1:2) required a long time (approximately 490 s) for gelation, which is too slow for in vivo applications. Additionally, the powder hydrogel with a higher gelatin ratio exhibited a higher modulus (Fig. 3D). We further examined gel stability by incubating the prepared powder hydrogels in PBS. Powder (1:8) and powder (1:16) hydrogels were unstable and degraded in PBS in 7 days, whereas the powder (1:2) and powder (1:4) hydrogels remained intact with good stability (Fig. S5). Such instability may be attributed to insufficient crosslinking (Schiff base formation between gelatin and dex-ald). Aldehyde groups were densely located in the dex-ald chains (0.58 aldehyde groups per glucose unit), which appear to ineffectively react with the amine groups in gelatin due to steric hindrance. Thus, an aldehyde content higher than the amine content is required to form a stable crosslinked hydrogel. The powder (1:4) contained 3.3 times more amine groups than aldehyde groups (Fig. 3E). Based on the gelation time, modulus, and stability, the powder (1:4) hydrogel was determined to be the most suitable as an in situ-forming powder hydrogel.

3.3. Tissue-adhesion of dex-ald/gelatin powder hydrogel

The tissue adhesion of the powder hydrogels with different dex-ald/gelatin ratios (1:2, 1:4, 1:8, and 1:16) was evaluated by a lap shear test using porcine skin tissues (Fig. 4A). The powder hydrogels demonstrated higher adhesion strength (7.5–15.2 kPa) compared to commercial fibrin glue (2.8 kPa) (Fig. 4B). The strong tissue adhesion of the powder hydrogels may be attributed to both covalent and noncovalent bonds at the tissue/hydrogel interfaces. The aldehyde group in dex-ald can form a covalent Schiff base with the amine group present in the tissue, which primarily contributes tissue adhesion. Powder hydrogels with a high gelatin ratio (≥1:4) exhibited significantly higher adhesive strength than the powder (1:2) hydrogel (7.5 kPa). This observation suggests that gelatin possessing various functional groups (e.g., amine, carboxyl, and hydroxyl groups) that can interact with tissues via non-covalent interactions can enhance tissue adhesion [30–33]. For instance, the adhesion strengths of dextran/gelatin and gelatin powder hydrogels were 24 % and 17 %, respectively, of that of the dex-ald/gelatin powder (1:4) hydrogel on skin tissue (Fig. S6). Adhesion strength of the powder (1:4) hydrogel to pig skin gradually increased after PBS addition (Fig. S7), indicating a continuous reaction between the hydrogel and the skin. Notably, dex-ald/gelatin powder hydrogels also adhered firmly to various ex vivo mouse organs (i.e., muscle, spleen, lung, kidney, heart, and liver), demonstrating their broad applicability (Fig. S8).

The powder (1:4) hydrogel exhibited stable tissue adhesion under various deformation conditions (bending and twisting) mimicking skeletal muscle movement in vivo (Fig. 4C). Moreover, the powder (1:4) hydrogel remained stable even after deformation in water and water flushing, suggesting excellent adhesion and stability in wet environments. Hence, the powder (1:4) hydrogel with strong and stable tissue adhesion was expected to be appropriate for skeletal muscle regeneration in VML.

We investigated additional factors potentially affecting the formation and properties of powder hydrogels. Because the powder on a tissue absorbs tissue fluid and/or buffer solution to different degrees, we studied the influence of the initial hydration volume on the properties of the resultant powder (1:4) hydrogel (e.g., stability, modulus, equilibrium water content [EWC], and tissue adhesion) (Fig. S9). Specifically, dex-ald/gelatin powder was hydrated with different PBS volumes, incubated at 37 °C for 3 h, and subjected to swelling by incubation in PBS for 1 d (Fig. S9A). The powder hydrogels formed with a small hydration volume (1 mL PBS/g powder) were mostly dissolved, leaving a low residual gel content (Fig. S9C). This result indicates insufficient hydration and substantial loss of the unhydrated powder. Therefore, sufficient hydration of the powder with an appropriate amount of fluid is necessary to form an intact powder hydrogel. However, hydration with 3 and 6 mL PBS (per g powder) did not lead to significant differences in the residual gel contents. The shear elastic modulus and EWC showed no significant differences among the powder hydrogel groups treated with different hydration volumes, implying that the powder hydrogels had similar crosslinking densities once gelation occurred (Figs. S9D and S9E). The highest tissue adhesion was observed for the powder hydrogel prepared using 3 mL PBS/g powder (Fig. S9F). The powder hydrogel prepared with 1 mL PBS/g powder had relatively low adhesion, likely due to incomplete hydrogel formation. The powder hydrogel prepared with a large hydration volume (6 mL PBS/g powder) had a relatively low adhesion strength, which may be due to the low density of the adhesive functional groups at the tissue interface.

Dex-ald in our powder hydrogel reacts with amine groups both in gelatin and on tissue surfaces for gelation and tissue adhesion,

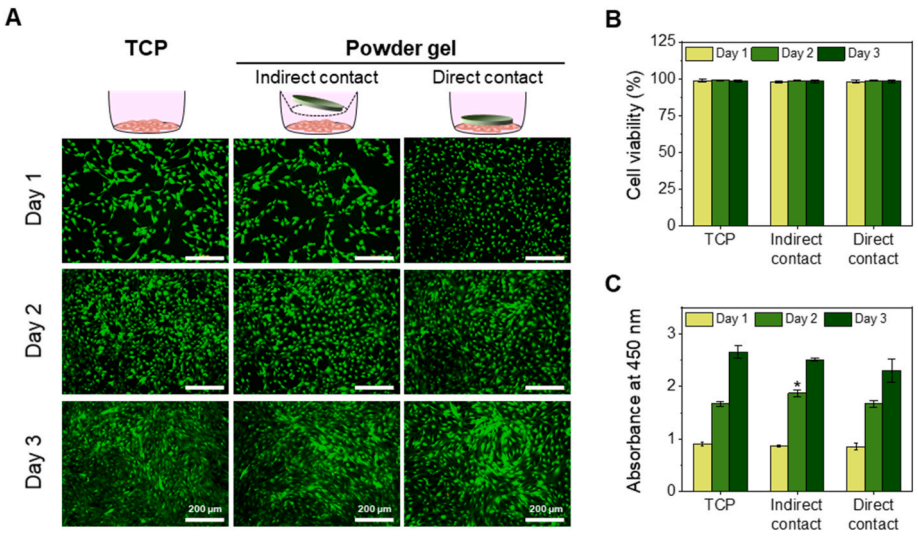

Fig. 5. In vitro cytocompatibility tests. (A) Live (green)/dead (red) staining of the C2C12s cultured on the tissue culture plate (TCP), with the powder hydrogel in a Transwell insert (indirect contact) or with the powder hydrogel (direct contact) on days 1, 2, and 3. (B) Cell viability and (C) metabolic activity in each group for 3 days. Cell viability was quantified using live/dead staining images. Metabolic activity was quantified by measuring the absorbance at a wavelength of 450 nm using the WST-1 assay. Statistical significance was analyzed by one-way ANOVA followed by a Tukey analysis. *$p < 0.05$ compared to day 2 metabolic activity of the cells culture on TCP.

respectively. To investigate the influence of tissue adhesion of the hydrogel on its mechanical strength, we prepared powder hydrogels on glass slides and pig skins, in which glass slides lacks amine groups and pig skins contains amine groups for reaction and measured their moduli (Fig. S10). We observed no significant difference in the moduli of the two hydrogels, indicating that tissue adhesion does not significantly influence gel strength (crosslinking). This may be because the amount of aldehyde groups in the powder was sufficiently higher than that of the amine groups in gelatin, allowing sufficient crosslinking even with reaction with tissue surfaces. In addition, the dex-ald is expected to react with the amine groups on tissue surfaces, to a much lesser extent, compared to those within gelatin for gelation. Moreover, we evaluated potential batch variation in adhesion strength by performing three independent tests (Fig. S11). The adhesion strengths in three tested

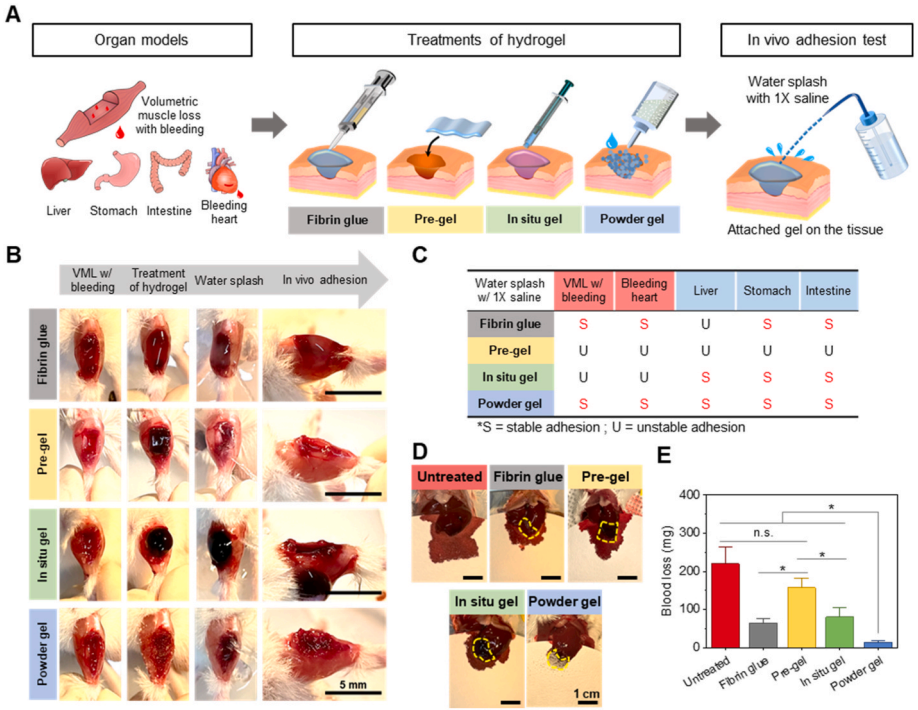

Fig. 6. In-vivo adhesion and hemostasis tests with various samples (fibrin glue, pre-formed hydrogel [pre-gel], in situ-formed hydrogel [in situ gel], and powder hydrogel [powder gel]) using various organs. (A) Schematic illustration of experimental procedures for tissue adhesion tests. (B) Photographs of various samples treated on VML-injured TA muscle during adhesion test. (C) Stability of samples for in vivo adhesion testing in organs from (B) and Supplementary Fig. S4. 'S' and 'U' stand for adhesion and unstable adhesion, respectively. (D) Various samples treated on mouse hemorrhagic liver. Photographs were acquired 3 min after sample treatment. Dotted line indicates each sample treated on hemorrhagic liver. (E) Blood loss in each group 3 min after sample treatment. Statistical significance was analyzed by one-way ANOVA followed by a Tukey analysis. *$p < 0.05$. n. s. Indicated no significant difference.

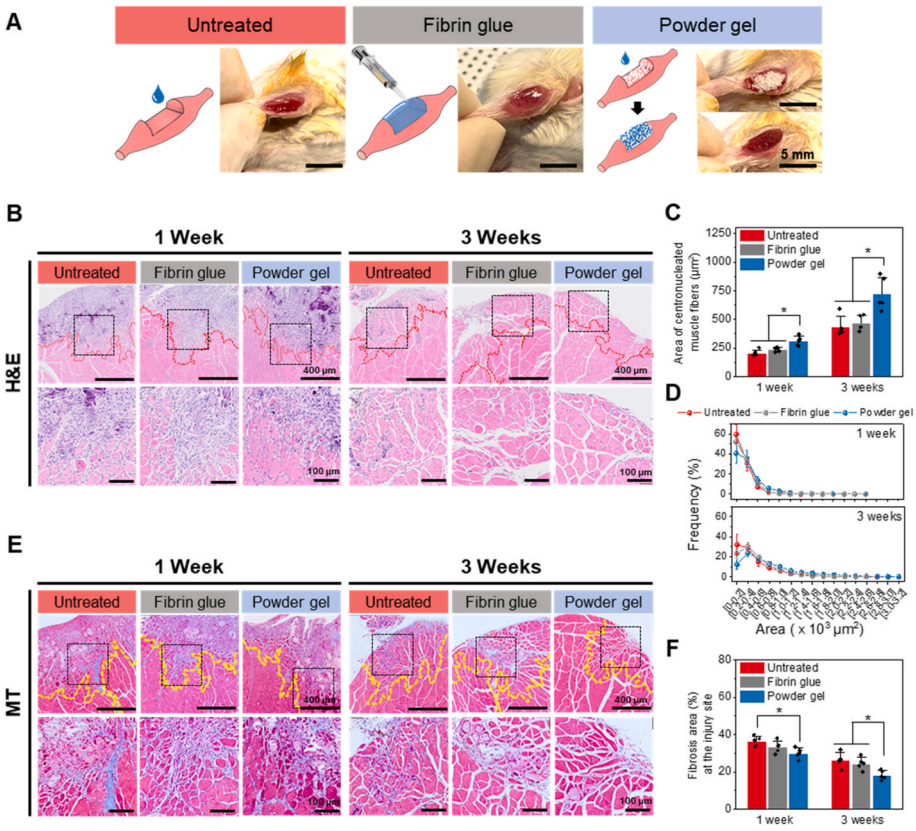

Fig. 7. In vivo skeletal muscle regeneration and scar tissue formation after VML injury and treatment of different samples. (A) Schematic illustrations and photographs of the experimental groups (untreated, fibrin glue, and powder hydrogel [powder gel]). (B) Representative hematoxylin and eosin (H&E) staining images of the tibialis anterior (TA) muscles at 1 and 3 weeks after VML injury and treatment. Red dotted lines indicate interfaces between injured tissues and regenerated tissues. (C) Average areas of centronucleated muscle fibers and (D) distributions of the areas of centronucleated muscle fibers at 1 and 3 weeks after VML injury and treatment. (E) Representative Masson's trichrome (MT) staining images of the TA muscles at 1 and 3 weeks after VML injury and treatment. Yellow-dotted lines indicate interfaces between injured tissues and regenerated tissues. (F) Area of fibrosis (%) at the injury site at 1 and 3 weeks after VML injury and treatment. Statistical significance was analyzed by one-way ANOVA followed by Tukey analysis. $^{*}p < 0.05$.

hydrogels were similar with no significant difference, indicating the robustness of the dex-ald/gel powder gel properties and handling procedures.

3.4. Cytocompatibility of the dex-ald/gelatin powder hydrogel

The cytocompatibility of the powder hydrogel was evaluated by culturing mouse C2C12 myoblasts in direct and indirect contact culture modes (Fig. 5). In both culture modes, cells cultured with the hydrogels were mostly viable with high cell viability (>97 %) on days 1, 2, and 3, which was not significantly different from that those cultured on tissue culture plates (TCP) (Fig. 5A and B). Furthermore, the metabolic activity was measured using a WST-1 assay for 3 days to investigate the effects of the powder hydrogel on cell proliferation (Fig. 5C). Similar to the control (TCP), C2C12 cells cultured with the powder hydrogel proliferated well in both indirect and direct contact modes for up to 3 days, and no significant difference in metabolic activity between the powder hydrogel and TCP groups was observed during the culture. These results suggested that our powder hydrogel did not impair cell viability or metabolic activity. The excellent cytocompatibility of the powder hydrogel may be associated with the inherent biocompatibility of the powder hydrogel components (gelatin and dextran) [33,34].

3.5. In vivo adhesion, hemostasis, and degradability of the dex-ald/gelatin powder hydrogel

We examined the feasibility of the dex-ald/gelatin powder hydrogel as a tissue-adhesive hydrogel for in vivo applications by examining its tissue adhesion, hemostasis ability, and degradability. Appropriate tissue adhesion of hydrogels is important for providing reliable connections between tissues subjected to dynamic movements, such as skeletal muscles, and for stably supporting tissue regeneration. We investigated the in vivo tissue adhesion of the powder (1:4) hydrogels and various controls (a pre-formed hydrogel, an in situ formed hydrogel, and commercial fibrin glue) and compared their characteristics (Fig. 6). Note that pre-formed and in situ formed hydrogels had the same composition as the powder hydrogel. We evaluated hydrogel samples using various organs, including bleeding organs (e.g., hemorrhagic mouse TA muscle with VML injury and hemorrhagic rat heart) and non-bleeding organs (rat liver, stomach, and intestine). Each hydrogel was subjected to water splashing on an organ to assess its adhesion and stability. In the hemorrhagic TA muscle with VML injury, the powder hydrogel and fibrin glue remained stable with good adhesion to the injured sites (Fig. 6B and C). In contrast, the pre-formed and in situ formed hydrogels were readily detached under identical conditions. In particular, the pre-formed hydrogel did not adhere to any organ. The in situ formed hydrogels adhered only to non-bleeding organs (Fig. 6C and S12). The results demonstrated that these types of hydrogels (pre-formed hydrogel and in situ formed hydrogel) are not suitable for treating wounds without dressings or sutures. Fibrin glue adhered stably to the bleeding organs; however, its adhesion to the liver was unstable, likely because of its smooth surface. In contrast, the powder hydrogels adhered to all organs, including the bleeding VML and the heart. The excellent tissue adhesiveness of our powder hydrogel is attributed to the fact that dried dex-ald/gelatin powder can absorb interfacial biological fluid or blood from wounds and effectively interact with tissues.

Hemostasis is important for skeletal muscle regeneration. Skeletal muscle regeneration can be facilitated by a hemostatic material that allows rapid blood uptake, coagulation factor enrichment, strong tissue adhesion, and physical protection of the injured muscle [35,36]. In our study, the in vivo hemostatic abilities of fibrin glue, pre-formed hydrogel, in situ-formed hydrogel, and dex-ald/gelatin powder (1:4) were assessed using a mouse hemorrhagic liver model (Fig. 6D and E). Without any treatment (control), a substantial blood loss (220 ± 35 mg) was observed. Similarly, treatment with the pre-formed hydrogel did not reduce blood loss (157 ± 20 mg). Blood loss was significantly reduced in the fibrin glue (65 ± 8 mg) and in situ-formed hydrogel (80 ± 21 mg). Importantly, the lowest blood loss (14 ± 4 mg) was observed from the powder hydrogel group, confirming that the dex-ald/gelatin powder had excellent hemostatic ability beneficial for would healing.

The powder hydrogels also exhibited excellent hemocompatibility, characterized as minimal hemolytic activity, improved blood coagulability, and minimal interference in blood clotting pathways (Fig. S13, S14 and S15). In particular, the powder gel demonstrated superior blood coagulability with a lower blood clotting index compared to the other tested samples, including PBS, a pre-formed hydrogel, an in situ formed hydrogel, and commercial fibrin glue. Dex-ald and gelatin, released from the powder at the interface with blood, might effectively capture red blood cells and platelets and induce the aggregation via diverse mechanisms, such as chemical bonding between the aldehyde groups of dex-ald and the amine groups on the red blood cells, hydrogen bonding, and electrostatic interactions. In addition, the powder did not adversely affect either intrinsic or extrinsic blood clotting pathways, as assessed by prothrombin time (PT) and activated partial thromboplastin time (aPTT) tests. Dex-ald/gelatin powder had PT (20.0 ± 0.6 s) and aPTT (24.8 ± 1.2 s) similar to control, falling within the normal coagulation time ranges for Sprague-Dawley rats [37]. Interestingly, the bursting pressure test using porcine small intestine revealed that the dex-ald/gel powder hydrogel showed the highest value (10.4 ± 1.3 kPa) compared to fibrin glue (6.2 ± 1.5 kPa), pre-gel (0.9 ± 0.3 kPa), and in situ gel (2.9 ± 0.75 kPa) (Fig. S16). This superior performance in burst resistance might be attributed to strong tissue adhesiveness and high mechanical strength of the powder hydrogel.

Biodegradable hydrogels are favored in tissue engineering because they can support tissue regrowth during tissue repair and disappear after tissue regeneration [5,38]. Incubation of the hydrogels in PBS led to dissociation and content loss, which was dependent on incubation time after hydration, indicating their biodegradability (Fig. S17). Furthermore, the in vivo biodegradability of the powder hydrogels (dex--ald/gelatin powder (1:4) containing a trace amount of Cy5-conjugated gelatin) was investigated by subcutaneous implantation in mice to monitor the fluorescence intensity at the implantation site (Fig. S18). The fluorescence intensity decreased substantially after implantation and became minimal on day 21 (Fig. S18). These results imply that our biodegradable powder hydrogel can initially support hemostasis, tissue adhesion/integration, and regeneration, and then gradually degrade, allowing for muscle tissue ingrowth and regeneration. Altogether, we demonstrated the promising characteristics of dex-ald/gelatin powder hydrogels (in vivo tissue adhesion, hemostasis, and degradation) suitable for skeletal muscle regeneration.

3.6. *In vivo skeletal muscle regeneration using the dex-ald/gelatin powder hydrogel*

The efficacy of the dex-ald/gelatin powder (1:4) hydrogel for skeletal muscle regeneration after VML injury was examined by histological analyses of the TA muscles 1 and 3 weeks after VML and hydrogel treatment (Fig. 7A). We included an untreated group and a fibrin glue-treated group as controls. Distinct regenerated tissue covering the defect was found in the powder gel group at 1 and 3 weeks, which was larger than those in the untreated and fibrin glue groups (Fig. 7B). Centronucleated muscle fibers in the TA muscle after VML have primarily been analyzed as indicators of muscle regeneration [39]. The areas of regenerated muscle fibers at 1 and 3 weeks were significantly higher in the powder hydrogel group than those in the fibrin glue and untreated groups (Fig. 7C). For example, the average areas of regenerated muscle fibers within the injured area were 209 ± 23, 237 ± 14, and 304 ± 39 μm^2 at 1 week and 438 ± 80, 468 ± 58, and 703 ± 127 μm^2 at 3 weeks for the untreated, fibrin glue, and powder hydrogel groups, respectively. In addition, in the H&E image at 1 week, more cells infiltrated the powder hydrogel in the regenerating tissue region than in the other groups (Fig. S20), suggesting that the powder hydrogels induced muscle cell growth and infiltration for regeneration, with appropriate degradation. The implanted powder hydrogel remained at the site at 1 week, but no hydrogel was found at 3 weeks, indicating the degradation of the implanted powder hydrogel during muscle regeneration (Fig. S20). The distribution of the regenerated muscle fiber areas at 1 and 3 weeks indicated a greater population of large fibers in the powder hydrogel group than in the untreated and fibrin glue groups (Fig. 7D). These results demonstrated that the powder hydrogels significantly facilitated muscle regeneration after VML injury. Scar tissue formation was evaluated by analyzing collagen deposition in Masson's trichrome staining images (Fig. 7E). Muscle strength recovery was further evaluated using the TA muscles harvested at week 3 post implantation (Supplementary Fig. S21). The powder gel group showed the greatest recovery of TA muscle strength compared to other groups, while fibrin glue treatment also promoted muscle strength recovery compared to the untreated control. For example, the muscle strength recovery was 38.2 ± 5.5 %, 53.6 ± 11.0 %, and 89.0 ± 5.5 % for untreated, fibrin glue, and powder gel groups, respectively. This improvement of functional muscle strength recovery correlated well with the trends observed in histological evaluation (e.g., centonucleated muscle fiber areas).

Insufficient or improper muscle regeneration is typically accompanied by pathological tissue remodeling and fibrosis [7,40]. One week after VML injury and treatment, the area of fibrosis was significantly reduced in the powder hydrogel group compared to that in the untreated group (Fig. 7F). After 3 weeks, decreases in fibrotic areas were observed in all groups, and the fibrotic area was smaller than that in the control groups. For example, the fibrosis areas in 3 weeks were 26.3 ± 3.5 %, 24.5 ± 2.9 %, and 18.9 ± 2.4 % for the untreated, fibrin glue, and powder hydrogel groups, respectively. To further investigate fibrosis tissue formation, we performed Picro-sirius red staining and α-smooth muscle actin (α-SMA) immunostaining to assess pathological collagen (type I and III) deposition and myofibroblast activation, respectively (Fig. S22). Our powder hydrogel group substantially reduced the pathological collagen deposition and α-SMA expression compared to untreated and fibrin glue groups. These results indicate that powder hydrogel treatment, offering strong tissue adhesion and mechanical support, can substantially promote skeletal muscle regeneration with reduced scar tissue after VML injury.

In addition to a sufficient supply of oxygen and nutrients [39], vascularization can activate resident satellite cells and facilitate the migration of muscle progenitor cells to injury sites for muscle regeneration [40]. Hence, vascularization in sample-treated muscle tissues was analyzed to assess skeletal muscle regeneration. The powder hydrogel group showed increased neovessel formation in the injured tissue compared to the untreated group after 1 week of treatment (Fig. 8A and S23A). After 3 weeks, vascularization further increased in all groups, and vascularization was higher in the powder hydrogel groups than that in the untreated and fibrin glue groups. Moreover, we examined inflammatory tissue reactions at the injury sites by immunostaining of tissue macrophages because macrophages play key roles in inflammation. Macrophages can induce or resolve inflammation depending on their microenvironment. Macrophages polarize themselves into inflammatory (M1) or anti-inflammatory (M2) phenotypes [40]. Excessive numbers of inflammatory macrophages amplify inflammation and induce scar tissue formation [41,42]. In our study, the phenotypes of macrophages at the VML injury sites were assessed by double staining

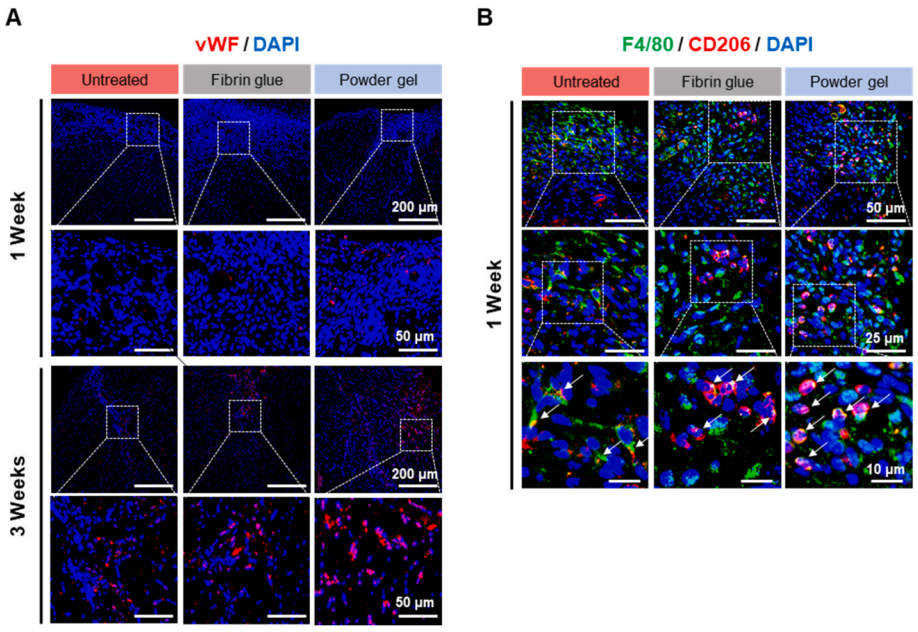

Fig. 8. Representative immunofluorescence images of tibialis anterior (TA) muscle after VML injury and treatment. (A) Immunofluorescence staining of von Willebrand factor (vWF, an endothelial marker, red) in the injured site at 1 and 3 weeks. (B) Immunofluorescence staining of F4/80 (a pan-macrophage marker, green) and CD206 (an anti-inflammatory macrophage marker, red) in the injured site at 1 week. Arrows indicate co-localization (yellow) of F4/80 and CD206 signals.

for F4/80 (a pan-macrophage marker) and CD206 (an anti-inflammatory macrophage marker) (Fig. 8B). After 1 week of treatment, the powder hydrogel group showed a significantly higher frequency of F4/80 (+)/CD206 (+) cells than the other groups. The powder hydrogel more effectively induced macrophage polarization toward an anti-inflammatory phenotype at the injury site than the untreated and fibrin glue groups (Fig. S23B). Anti-inflammatory (M2) macrophages can facilitate myoblast growth and differentiation, and enhance skeletal muscle regeneration [40,43]. Altogether, the powder hydrogel treatment promoted angiogenesis and anti-inflammatory tissue responses, which led to improved skeletal muscle regeneration with reduced scar tissue.

4. Conclusion

We successfully developed wet-adhesive powders that could absorb wound interfacial water and form hydrogels with strong tissue adhesion using biocompatible and biodegradable dex-ald and gelatin. The dex-ald/gelatin powder, composed of a 1:4 (dex-ald:gelatin) ratio, displayed characteristics beneficial for skeletal muscle regeneration, such as strong adhesion to the wound site even in a wet environment, mechanical support, hemostasis, and degradability. The powder hydrogel significantly improved skeletal muscle regeneration and reduced scar tissue formation. Immunohistological analyses revealed that the powder hydrogel induced angiogenesis and anti-inflammatory macrophage polarization in the VML-injured skeletal muscle. Overall, our dex-ald/gelatin powder hydrogel demonstrated notable efficacy in facilitating skeletal muscle regeneration in VML injury and will serve as a promising platform for the development of biomaterial-based regeneration strategies for various tissues.

Ethics approval and consent to participate

All subjects gave their informed consent for inclusion before they participated in the study. All participants reviewed the methodological, ethical, legal and societal issues involved in the research and in the uses of animal study. All animal study was performed with approval from the Gwangju Institute of Science and Technology Institutional Animal Care and Use Committee (study approval number: GIST-2023-041), and all experiments were performed after approval by a local ethics committee at Gwangju Institute of Science and Technology.

Data availability statement

The data that support the findings of this study are available from the corresponding author upon reasonable request.

CRediT authorship contribution statement

Mingyu Lee: Writing – review & editing, Writing – original draft, Visualization, Methodology, Investigation. **Daun Seo:** Methodology, Investigation, Writing – original draft, Writing – review & editing, Visualization. **Junggeon Park:** Methodology, Investigation. **Sun Hong Lee:** Methodology, Investigation. **Jin Jeon:** Methodology, Investigation. **Woochan Kim:** Investigation, Methodology. **Jangho Kim:** Methodology, Resources, Supervision. **Hee Seok Yang:** Supervision, Resources, Methodology. **Jae Young Lee:** Writing – review & editing, Supervision, Resources, Methodology, Funding acquisition, Conceptualization.

Declaration of competing interest

The authors declare that they have no known competing financial interests or personal relationships that could have appeared to influence the work reported in this paper.

Acknowledgements

This work was supported by a grant from the National Research Foundation of Korea (NRF) funded by the Ministry of Science, ICT, and Future Planning (2021M3H4A1A04092882 and 2023R1A2C2002802).

Appendix A. Supplementary data

Supplementary data to this article can be found online at https://doi.org/10.1016/j.bioactmat.2024.06.017.

References

[1] C. Nelke, R. Dziewas, J. Minnerup, S.G. Meuth, T. Ruck, Skeletal muscle as potential central link between sarcopenia and immune senescence, EBioMedicine 49 (2019) 381–388, https://doi.org/10.1016/j.ebiom.2019.10.034.

[2] W.R. Frontera, J. Ochala, Skeletal muscle: a brief review of structure and function, Calcif. Tissue Int. 96 (2015) 183–195, https://doi.org/10.1007/s00223-014-9915-y.

[3] M. Juhas, N. Bursac, Engineering skeletal muscle repair, Curr. Opin. Biotechnol. 24 (2013) 880–886, https://doi.org/10.1016/j.copbio.2013.04.013.

[4] Y. Zhao, S. Song, X. Ren, J. Zhang, Q. Lin, Y. Zhao, Supramolecular adhesive hydrogels for tissue engineering applications, Chem. Rev. 122 (2022) 5604–5640, https://doi.org/10.1021/acs.chemrev.1c00815.

[5] J.M. Grasman, M.J. Zayas, R.L. Page, G.D. Pins, Biomimetic scaffolds for regeneration of volumetric muscle loss in skeletal muscle injuries, Acta Biomater. 25 (2015) 2–15, https://doi.org/10.1016/j.actbio.2015.07.038.

[6] M. Shi, R. Dong, J. Hu, B. Guo, Conductive self-healing biodegradable hydrogel based on hyaluronic acid-grafted-polyaniline as cell recruitment niches and cell delivery carrier for myogenic differentiation and skeletal muscle regeneration, Chem. Eng. J. 457 (2023) 141110, https://doi.org/10.1016/j.cej.2022.141110.

[7] N. Narayanan, Z. Jia, K.H. Kim, L. Kuang, P. Lengemann, G. Shafer, V. Bernal-Crespo, S. Kuang, M. Deng, Biomimetic glycosaminoglycan-based scaffolds improve skeletal muscle regeneration in a Murine volumetric muscle loss model, Bioact. Mater. 6 (2021) 1201–1213, https://doi.org/10.1016/j.bioactmat.2020.10.012.

[8] B.M. Sicari, J.P. Rubin, C.L. Dearth, M.T. Wolf, F. Ambrosio, M. Boninger, N. J. Turner, D.J. Weber, T.W. Simpson, A. Wyse, E.H.P. Brown, J.L. Dziki, L.E. Fisher, S. Brown, S.F. Badylak, An acellular biologic scaffold promotes skeletal muscle formation in mice and humans with volumetric muscle loss, Sci. Transl. Med. 6 (2014), https://doi.org/10.1126/scitranslmed.3008085, 234ra58-234ra58.

[9] P. Bertsch, M. Diba, D.J. Mooney, S.C.G. Leeuwenburgh, Self-healing injectable hydrogels for tissue regeneration, Chem. Rev. 123 (2023) 834–873, https://doi.org/10.1021/acs.chemrev.2c00179.

[10] Y. Yi, C. Xie, J. Liu, Y. Zheng, J. Wang, X. Lu, Self-adhesive hydrogels for tissue engineering, J. Mater. Chem. B 9 (2021) 8739–8767, https://doi.org/10.1039/D1TB01503F.

[11] Y. Xu, C. Xu, K. Yang, L. Ma, G. Li, Y. Shi, X. Feng, L. Tan, D. Duan, Z. Luo, C. Yang, Copper Ion-Modified Germanium Phosphorus Nanosheets Integrated with an Electroactive and Biodegradable Hydrogel for Neuro-Vascularized Bone Regeneration, Adv. Healthcare Mater. n/a (n.d.) 2301151. https://doi.org/10.1002/adhm.202301151.

[12] M. Lee, J. Park, G. Choe, S. Lee, B.G. Kang, J.H. Jun, Y. Shin, M.C. Kim, Y.S. Kim, Y. Ahn, J.Y. Lee, A conductive and adhesive hydrogel composed of MXene nanoflakes as a paintable cardiac patch for infarcted heart repair, ACS Nano 17 (2023) 12290–12304, https://doi.org/10.1021/acsnano.3c00933.

[13] B. Guo, Y. Liang, R. Dong, Physical dynamic double-network hydrogels as dressings to facilitate tissue repair, Nat. Protoc. (2023) 1–33, https://doi.org/10.1038/s41596-023-00878-9.

[14] J. Park, T.Y. Kim, Y. Kim, S. An, K.S. Kim, M. Kang, S.A. Kim, J. Kim, J. Lee, S.-W. Cho, J. Seo, A Mechanically Resilient and Tissue-Conformable Hydrogel with Hemostatic and Antibacterial Capabilities for Wound Care, Adv. Sci. n/a (n.d.) 2303651. https://doi.org/10.1002/advs.202303651.

[15] M. Lee, M.C. Kim, J.Y. Lee, Nanomaterial-based electrically conductive hydrogels for cardiac tissue repair, Int. J. Nanomed. 17 (2022) 6181–6200, https://doi.org/10.2147/IJN.S386763.

[16] H. Yuk, C.E. Varela, C.S. Nabzdyk, X. Mao, R.F. Padera, E.T. Roche, X. Zhao, Dry double-sided tape for adhesion of wet tissues and devices, Nature 575 (2019) 169–174, https://doi.org/10.1038/s41586-019-1710-5.

[17] L. Han, M. Wang, L.O. Prieto-López, X. Deng, J. Cui, Self-hydrophobization in a dynamic hydrogel for creating nonspecific repeatable underwater adhesion, Adv. Funct. Mater. 30 (2020) 1907064, https://doi.org/10.1002/adfm.201907064.

[18] X. Peng, X. Xia, X. Xu, X. Yang, B. Yang, P. Zhao, W. Yuan, P.W.Y. Chiu, L. Bian, Ultrafast self-gelling powder mediates robust wet adhesion to promote healing of gastrointestinal perforations, Sci. Adv. 7 (2021) eabe8739, https://doi.org/10.1126/sciadv.abe8739.

[19] Y. Fang, L. Zhang, Y. Chen, S. Wu, Y. Weng, H. Liu, Polysaccharides based rapid self-crosslinking and wet tissue adhesive hemostatic powders for effective hemostasis, Carbohydr. Polym. 312 (2023) 120819, https://doi.org/10.1016/j.carbpol.2023.120819.

[20] B. Li, H. Li, H. Chen, Y. Liu, J. Chen, Q. Feng, X. Cao, H. Dong, Microgel assembly powder improves acute hemostasis, antibacterial, and wound healing via in situ Co-assembly of erythrocyte and microgel, Adv. Funct. Mater. 33 (2023) 2302793, https://doi.org/10.1002/adfm.202302793.

[21] Y. Du, X. Chen, L. Li, H. Zheng, A. Yang, H. Li, G. Lv, Benzeneboronic−alginate/quaternized chitosan−catechol powder with rapid self-gelation, wet adhesion, biodegradation and antibacterial activity for non-compressible hemorrhage control, Carbohydr. Polym. 318 (2023) 121049, https://doi.org/10.1016/j.carbpol.2023.121049.

[22] D. Zhang, R. Chang, Y. Ren, Y. He, S. Guo, F. Guan, M. Yao, Injectable and reactive oxygen species-scavenging gelatin hydrogel promotes neural repair in experimental traumatic brain injury, Int. J. Biol. Macromol. 219 (2022) 844–863, https://doi.org/10.1016/j.ijbiomac.2022.08.027.

[23] J. Park, J. Jeon, B. Kim, M.S. Lee, S. Park, J. Lim, J. Yi, H. Lee, H.S. Yang, J.Y. Lee, Electrically conductive hydrogel nerve guidance conduits for peripheral nerve regeneration, Adv. Funct. Mater. 30 (2020) 2003759, https://doi.org/10.1002/adfm.202003759.

[24] A.H. Fischer, K.A. Jacobson, J. Rose, R. Zeller, Hematoxylin and eosin staining of tissue and cell sections, Cold Spring Harb. Protoc. 2008 (2008), https://doi.org/10.1101/pdb.prot4986 pdb.prot4986.

[25] Y. Fu, J. Zhang, Y. Wang, J. Li, J. Bao, X. Xu, C. Zhang, Y. Li, H. Wu, Z. Gu, Reduced polydopamine nanoparticles incorporated oxidized dextran/chitosan hybrid hydrogels with enhanced antioxidative and antibacterial properties for accelerated wound healing, Carbohydr. Polym. 257 (2021) 117598, https://doi.org/10.1016/j.carbpol.2020.117598.

[26] L. Li, J. Ge, P.X. Ma, B. Guo, Injectable conducting interpenetrating polymer network hydrogels from gelatin- graft -polyaniline and oxidized dextran with enhanced mechanical properties, RSC Adv. 5 (2015) 92490–92498, https://doi.org/10.1039/C5RA19467A.

[27] D. Shen, Q. Hu, J. Sun, X. Pang, X. Li, Y. Lu, Effect of oxidized dextran on the stability of gallic acid-modified chitosan–sodium caseinate nanoparticles, Int. J. Biol. Macromol. 192 (2021) 360–368, https://doi.org/10.1016/j.ijbiomac.2021.09.209.

[28] M. Shin, K.H. Song, J.C. Burrell, D.K. Cullen, J.A. Burdick, Injectable and conductive granular hydrogels for 3D printing and electroactive tissue support, Adv. Sci. 6 (2019) 1901229, https://doi.org/10.1002/advs.201901229.

[29] D.B. Emiroglu, A. Bekcic, D. Dranseike, X. Zhang, T. Zambelli, A.J. deMello, M. W. Tibbitt, Building block properties govern granular hydrogel mechanics through contact deformations, Sci. Adv. 8 (2022) eadd8570, https://doi.org/10.1126/sciadv.add8570.

[30] K. Gelse, E. Pöschl, T. Aigner, Collagens—structure, function, and biosynthesis, Adv. Drug Deliv. Rev. 55 (2003) 1531–1546, https://doi.org/10.1016/j.addr.2003.08.002.

[31] S. Rose, A. Prevoteau, P. Elzière, D. Hourdet, A. Marcellan, L. Leibler, Nanoparticle solutions as adhesives for gels and biological tissues, Nature 505 (2014) 382–385, https://doi.org/10.1038/nature12806.

[32] Y. Mosleh, M. van Die, W. Gard, I. Breebaart, J.-W. van de Kuilen, P. van Duin, J. A. Poulis, Hygrothermal ageing of dry gelatine adhesive films: microstructure-property relationships, Int. J. Adhesion Adhes. 131 (2024) 103654, https://doi.org/10.1016/j.ijadhadh.2024.103654.

[33] N. Davidenko, C.F. Schuster, D.V. Bax, R.W. Farndale, S. Hamaia, S.M. Best, R. E. Cameron, Evaluation of cell binding to collagen and gelatin: a study of theeffect of 2D and 3D architecture and surface chemistry, J. Mater. Sci. Mater. Med. 27 (2016) 148, https://doi.org/10.1007/s10856-016-5763-9.

[34] S. Guan, K. Zhang, L. Cui, J. Liang, J. Li, F. Guan, Injectable gelatin/oxidized dextran hydrogel loaded with apocynin for skin tissue regeneration, Biomater. Adv. 133 (2022) 112604, https://doi.org/10.1016/j.msec.2021.112604.

[35] X. Yang, W. Liu, N. Li, M. Wang, B. Liang, I. Ullah, A.L. Neve, Y. Feng, H. Chen, C. Shi, Design and development of polysaccharide hemostatic materials and their hemostatic mechanism, Biomater. Sci. 5 (2017) 2357–2368, https://doi.org/10.1039/C7BM00554G.

[36] X. Zhao, Z. Zhang, J. Luo, Z. Wu, Z. Yang, S. Zhou, Y. Tu, Y. Huang, Y. Han, B. Guo, Biomimetic, highly elastic conductive and hemostatic gelatin/rGO-based nanocomposite cryogel to improve 3D myogenic differentiation and guide in vivo skeletal muscle regeneration, Appl. Mater. Today 26 (2022) 101365, https://doi.org/10.1016/j.apmt.2022.101365.

[37] H. Tabata, S. Nakamura, T. Matsuzawa, Some species differences in the false prolongation of prothrombin times and activated partial thromboplastin times in toxicology, Comp. Haematol. Int. 5 (1995) 140–144, https://doi.org/10.1007/BF00638933.

[38] M. Lee, Y.S. Kim, J. Park, G. Choe, S. Lee, B.G. Kang, J.H. Jun, Y. Shin, M. Kim, Y. Ahn, J.Y. Lee, A paintable and adhesive hydrogel cardiac patch with sustained release of ANGPTL4 for infarcted heart repair, Bioact. Mater. 31 (2024) 395–407, https://doi.org/10.1016/j.bioactmat.2023.08.020.

[39] M.M. Carleton, M. Locke, M.V. Sefton, Methacrylic acid-based hydrogels enhance skeletal muscle regeneration after volumetric muscle loss in mice, Biomaterials 275 (2021) 120909, https://doi.org/10.1016/j.biomaterials.2021.120909.

[40] N.J. Turner, S.F. Badylak, Regeneration of skeletal muscle, Cell Tissue Res. 347 (2012) 759–774, https://doi.org/10.1007/s00441-011-1185-7.

[41] W. Xiao, Y. Liu, P. Chen, Macrophage depletion impairs skeletal muscle regeneration: the roles of pro-fibrotic factors, inflammation, and oxidative stress, Inflammation 39 (2016) 2016–2028, https://doi.org/10.1007/s10753-016-0438-8.

[42] Y. Oishi, I. Manabe, Macrophages in inflammation, repair and regeneration, Int. Immunol. 30 (2018) 511–528, https://doi.org/10.1093/intimm/dxy054.

[43] J.G. Tidball, Mechanisms of muscle injury, repair, and regeneration, in: Compr. Physiol., John Wiley & Sons, Ltd, 2011, pp. 2029–2062, https://doi.org/10.1002/cphy.c100092.